Three-dimensional stimulation and imaging-based functional optical microscopy of biological cells

Quan, Xiangyu ; Kumar, Manoj ; Matoba, Osamu ; Awatsuji, Yasuhiro ; Hayasaki, Yoshio ; Hasegawa, Satoshi ; Wake, Hiroaki

(Citation)
Optics Letters,43(21):5447-5450

(Issue Date)
2018-11-01

(Resource Type)
journal article

(Version)
Accepted Manuscript

3D Stimulation and Imaging-based Functional Optical Microscopy (SIFOM) of Biological Cells

XIANGYU QUAN, [1,*] MANOJ KUMAR, [1] OSAMU MATOBA, [1] YASUHIRO AWATSUJI, [2] YOSHIO HAYASAKI, [3] SATOSHI HASEGAWA, [3] AND HIROAKI WAKE[4]

[1]Graduate School of System Informatics, Kobe University, Rokkodai 1-1, Nada, Kobe 657-8501, Japan
[2] Faculty of Electrical Engineering and Electronics, Kyoto Institute of Technology, Matsugasaki, Sakyo-ku, Kyoto 606-8585, Japan
[3] Center for Optical Research and Education (CORE), Utsunomiya University, 7-1-2 Yoto, Utsunomiya, 321-8585, Japan
[4] Division of System Neuroscience, Kobe University Graduate School of Medicine, Kusunoki-cho 7-5-1, Chuo-ku, Kobe, 650-0017, Japan
*Corresponding author: zen@rabbit.kobe-u.ac.jp

Received XX Month XXXX; revised XX Month, XXXX; accepted XX Month XXXX; posted XX Month XXXX (Doc. ID XXXXX); published XX Month XXXX

A new type of functional optical microscope system called three-dimensional (3D) stimulation and imaging-based functional optical microscopy (SIFOM) is proposed. SIFOM can precisely stimulate user-defined targeted biological cells and can simultaneously record the volumetric fluorescence distribution in a single acquisition. Precise and simultaneous stimulation of fluorescent-labeled biological cells is achieved by multiple 3D spots generated by digital holograms displayed on a phase-mode spatial light modulator. Single-shot 3D acquisition of the fluorescence distribution is accomplished by common-path off-axis incoherent digital holographic microscopy in which a diffraction grating with a focusing lens is displayed on another phase-mode spatial light modulator. The effectiveness of the proposed functional microscope system was verified in experiments using fluorescent microbeads and human lung cancer cells located at various defocused positions. The system can be used for manipulating the states of cells in optogenetics. © 2018 Optical Society of America

http://dx.doi.org/10.1364/OL.99.099999

In recent decades, in addition to their conventional role as observation tools, microscopes have evolved into manipulation tools and measurement tools for biological applications. For instance, in optogenetics, microscopes provide new ways to switch on and off a defined circuit of neurons with the help of photoactive proteins in the membrane [1-5]. High-speed, precise time control of the cells' patterns of firing of action potentials can be attained by using safe pulses of visible light [6]. Usually this process is achieved by using optical fibers or an optical window above the target region. One challenge in conventional optogenetics is that cell control is typically performed over a wide area. Two-dimensional (2D) illumination using imaging optics is an alternative tool for exciting functionally and locally defined specific cells. To further understand neural activity, three-dimensional (3D) multi-spot illumination and observation systems having millisecond-order precision are required. A high-speed 3D illumination and imaging system can be used to realize the design of neural circuits with unprecedented freedom.

In this letter, we propose a new type of optical microscope system called 3D stimulation and imaging-based functional optical microscopy (SIFOM). Fig. 1 conceptually shows the functions achievable by SIFOM, which can realize optogenetic neuronal stimulation and monitoring at the same time. There are two key functions of SIFOM: The first is programable stimulation of cells located in 3D space. The second is holographic 3D observation of the fluorescence distribution. Precise stimulation of the target cells is only possible if a 3D map of the cells is created. How to create a 3D map of cells and instantaneously observe the changes in cell status after stimulation is an important question that can lead to new discoveries. For instance, such a high-speed imaging and stimulation tool can monitor cell status within the circuit dynamics, and can accurately bring about action potentials at the right time and location to reinforce or inhibit signal transmission. A 3D map can be created in advance by using confocal microscopy. Bovetti and Fellin proposed a system based on confocal microscopy and 3D stimulation for neuron cell imaging that works in a sequential manner [7]. However, confocal microscopy is not an ideal approach for monitoring the stimulation reaction after or between stimulations due to the time-consuming sectioning process that it requires. To realize fast 3D recording, digital holographic techniques using incoherent light have been studied by many research groups [8-15]. For bioimaging applications, light efficiency is a very serious problem. We have proposed a common path off-axis digital holographic method to achieve high efficiency and single-shot recordings with a comparably simple configuration [14]. The recording speed is equal to that of typical wide-field imaging, and every frame of the hologram can reconstruct a whole

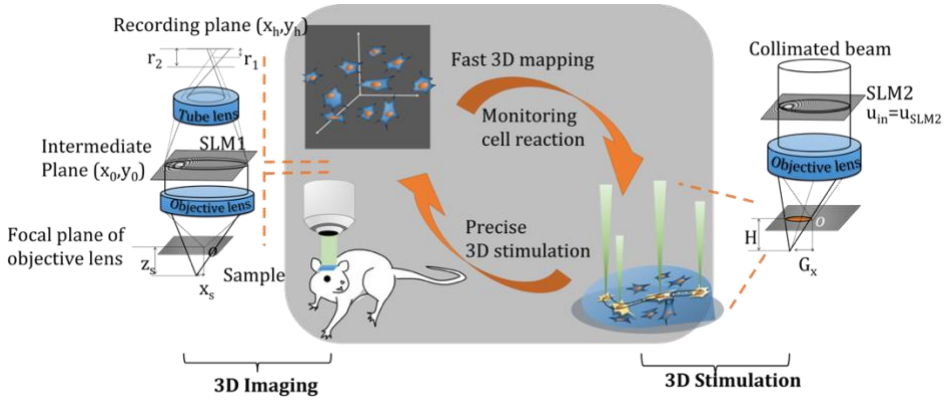

Fig. 1. Conceptual illustration of the functions of SIFOM in the case of in vivo brain stimulation and imaging experiments (center grey area), and schematic diagrams of 3D stimulation and imaging systems. SIFOM consists of an off-axis incoherent digital holographic microscopy system for 3D imaging (left), and a holographic multi-spot illumination system (right).

3D field image. Moreover, it is independent of the illumination. In the experiments described here, two fluorescent beads and cancer cells located at various defocused positions along the axial direction were recorded with the off-axis incoherent digital holographic method, and active multi-spot illumination selectively illuminated each bead or cell individually or all together, even at the out-of-focus positions. These results demonstrate the high potential of the proposed system.

Digital holographic 3D fluorescence imaging. We previously proposed a common-path off-axis incoherent digital holography technique, but the efficiency was not high due to interference between two diffracted waves [13]. Here, we propose an improved method by using the unmodulated transmitted fluorescence and tilted diffracted light with a slightly different wavefront curvature formed by a phase-mode spatial light modulator (SLM). A fluorescent object can be regarded as the superposition of quasi-point sources in the sample space. As shown on the left side in Fig. 1, light from the sth point source $\delta(x_s, y_s; z_s)$ has a quadratic phase distribution in an intermediate plane, described as

$$\boldsymbol{u_{Int}(x_0) = \exp\left(-\frac{i\pi x_0^2}{r_0\lambda}\right)\exp\left(-2i\pi x_0\frac{x_s}{f_{OL}\lambda}\right).} \quad \textbf{(1)}$$

Here, a one-dimensional axis, x_0, in the intermediate plane is considered. The radius of curvature of the objective beam is $r_0 = \frac{f_{OL}^2}{z_s}$, where f_{OL} is the focal length of the objective lens, and λ is the center wavelength. We used an SLM (SLM1 at left in Fig. 1) with a phase modulation function u_{SLM1} given by

$$\boldsymbol{u_{SLM1}(x_0) = \exp\left\{i \times tan^{-1}\left[\exp\left(\frac{-i\pi}{f_{SLM1}\lambda}x_0^2 + \frac{2i\pi x_0}{d_h}\right)\right]\right\}.} \quad \textbf{(2)}$$

The phase modulation function u_{SLM1} consists of a lens function with focal length f_{SLM1} and a diffraction grating function with grating period d_h.The part of the fluorescence with a polarization state parallel to the extraordinary axis of SLM1 is $u_{Int} \times u_{SLM1}$, whereas the polarization state perpendicular to the extraordinary axis remains unchanged as u_{Int}. At a recording plane, which is equivalent to the back focal plane (BFP) of the tube lens, the extraordinary ray u_{ex} and ordinary ray u_{or} are described as

$$\boldsymbol{u_{ex}(x_h) = \exp\left[\frac{i\pi}{\lambda r_1}\left(x_h + x_s M - \frac{f_{Tube}\lambda}{d_h}\right)^2\right],} \quad \textbf{(3)}$$

$$\boldsymbol{u_{or}(x_h) = exp\left[\frac{i\pi}{\lambda r_2}(x_h + x_s M)^2\right],} \quad \textbf{(4)}$$

where $r_1 = \frac{f_{Tube}^2}{f_{SLM1}} + z_s(\frac{f_{Tube}}{f_{OL}})^2$, $r_2 = z_s(\frac{f_{Tube}}{f_{OL}})^2$, and $M = \frac{f_{Tube}}{f_{OL}}$. Here, f_{Tube} is the focal length of the tube lens. By using a linear polarizer, it is possible to form holograms from those two beams. A hologram from a point source $\delta(x_s, y_s; z_s)$ makes part of a Fresnel zone plate with focal length $z_h = \pm\frac{r_1 r_2}{r_1 - r_2}$. Reconstructing the point source by Fresnel propagation yields the focused point source at an optimal reconstruction distance z_h.

Precise 3D stimulation. For typical wide-field epifluorescence imaging, the illumination light is focused on the focal plane of an objective lens, forming a collimated beam on the sample. In contrast, a collimated beam on the BFP forms a focused spot on the sample plane. Holographic multi-spot illumination with an SLM was proposed in the late 90s and was adopted in numerous applications [16-19]. In our SIFOM system, target cells and their 3D position can be manually or programmably defined from the previously obtained 3D map, and then the phase hologram is calculated and displayed on the phase-only spatial light modulator (SLM2 at right in Fig. 1).

As shown at the right side of Fig. 1, if the incoming wavefront u_{in} has a specific phase distribution, described as

$$\boldsymbol{u_{in}(x) = exp\left\{i \times tan^{-1}\left[\sum_k \exp\left(\frac{-i\pi x^2}{\lambda h_k}\right)\exp\left(\frac{i2\pi x}{g_{xk}}\right)\right]\right\}.} \quad \textbf{(5)}$$

after the objective lens, the wavefront at the front focal plane (FFP) becomes

$$\boldsymbol{u_{FFP}(X) = \sum_k \exp\left\{\frac{i\pi}{\lambda H_k}[(X - G_{xk})^2]\right\}.} \quad \textbf{(6)}$$

Here, $H_k = \frac{f_{OL}^2}{h_k}$, $G_{xk} = \frac{f_{OL}\lambda}{g_{xk}}$, and the kth focused spot falls on the position $(G_{xk}, G_{yk}; H_k)$ in the sample space. SLM2 can modulate the collimated incoming light to the desired phase distribution, pixel by pixel.

A schematic diagram of the functional optical microscope that includes the 3D multi-spot stimulation and 3D fluorescence imaging system is shown in Fig. 2. The left side shows the 3D fluorescence imaging system, and the right-side shows the 3D illumination system. The wavelength of the input illumination light in the 3D illumination system is 532 nm, and the output fluorescence is centered at 575 nm. Two SLMs are placed on the two sides of the

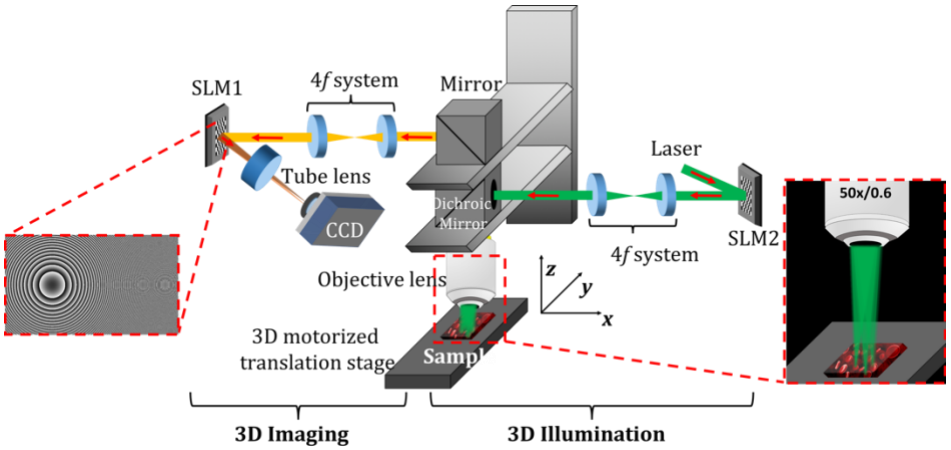

Fig. 2. Complete experimental set-up of SIFOM, containing 3D fluorescence imaging and 3D illumination microscope systems (SLM1: Holoeye pluto (1920×1080 pixels, 8 μm pixel pitch, phase-only modulation), SLM2: Hamamatsu Photonics (Hamamatsu X10468-01, 600 × 800 pixels, and 20 μm pixel pitch), Objective lens: x50, NA 0.6, CCD: Andor iXon,1024×1024, pixel size 13 μm).

microscope, as parts of the illumination system and the imaging system. A $4f$ relay system in the illumination part transmits the image of SLM2 to the BFP of the objective lens. Meanwhile, the zeroth order is blocked at an intermediate plane of the $4f$ system. Another SLM (SLM1) is also placed at the BFP of the objective lens by another $4f$ relay system in the imaging part. The Fourier transform of the object image is projected onto the plane of SLM1 and generates two distinct wavefronts at respective angles. The magnifications of the $4f$ relay systems in the illumination and imaging parts are adjusted by setting the aperture sizes of the objective lens and SLM2 to 0.5 and 1, respectively.

Experimental results. To verify the performance of the proposed system, experiments were performed using fluorescent beads and human lung cancer cells First, we demonstrated imaging of the fluorescent beads. The fluorescent beads (microspheres) used in the experiment had diameters of 10–14 μm. These beads were excited by green light (λ=532 nm) and emitted yellow fluorescence with wavelengths ranging from 550 nm to 600 nm. To improve the fringe visibility of the holograms, a bandpass filter centered at 575 nm$\pm$12.5 nm was placed in front of an EMCCD sensor. Two fluorescent beads were placed on the glass plate and were imaged, as shown in Fig. 3(a). Then, the glass plate was moved by a motorized translation stage in the z-direction by 80 μm. The hologram shown in Fig. 3(b) was obtained by displaying phase pattern $f_{SLM1} = 800$ mm and $d_h = 300$ μm on SLM1. Fig. 3(c) shows the reconstructed image obtained by applying $z_h = 950$ mm to the Fresnel propagation from the recorded hologram. In order to accurately illuminate each bead, we performed calibration by recording multiple illumination spots with known $(g_x, g_y; h \to \infty)$ on SLM2. By comparing the focused spots' positions (G_x, G_y) at the image sensor to the variables (g_x, g_y) on SLM2, a linear relationship between (g_x, g_y) and focus position (G_x, G_y) was obtained. This was performed prior to the experiments by putting a flat fluorescent plate on the focal plane of the objective lens. Figs. 3(d) and (e) show the holograms for selective illumination of each bead, and the respective reconstruction results. A similar experimental result is also made in movies in the supplementary materials. The signal-to-noise ratio (SNR) of the reconstructed images shown in Figs. 3(c), 3(d), and 3(e) were 24.87 dB, 29.96 dB, and 29.8 dB, respectively. The SNR is defined as the ratio of the mean value in the signal area to the noise area from a reconstructed image. It is easy to see that the SNR is improved with a controlled focal spot in the illumination.

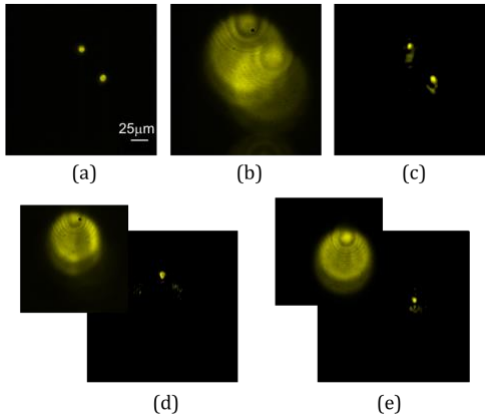

Fig. 3. Reconstruction of fluorescent beads. (a) Original focused image, (b) a hologram obtained by moving the beads 80 μm along the z-direction, (c) reconstructed beads, (d) selective illumination of an upper bead, (e) selective illumination of a lower bead (see Visualizations 1-3).

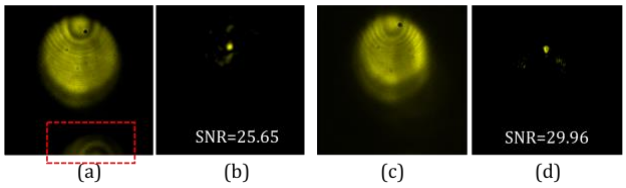

Fig. 4. Comparison of 3D illumination without depth information, showing (a) hologram and (b) reconstructed image, and with depth information applied to SLM2, showing (c) hologram and (d) reconstructed image.

Fig. 4 shows a comparison when patterns for $h \to \infty$ and $h = 80$ μm were applied to SLM2. When SLM2 displayed $h \to \infty$, as shown in Fig. 4(a), the illumination spot was under the position

where the bead was located. This caused noise from the adjacent bead, as shown in the red rectangular. It can be observed from Fig. 4(c) that the noise disappeared when depth information was applied to SLM2. It was also observed that the SNRs of the reconstructed images were improved.

The experiment was repeated for different axial positions from the same bead. In Fig. 5(a), the reconstructed depth positions are in good agreement with the theoretical values, z_h. Multiple beads on the same object plane are also reconstructed from a hologram, as shown in Figs. 5(b-d).

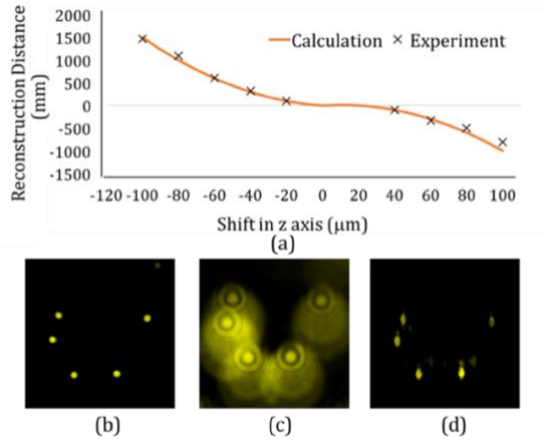

Fig. 5. (a) A plot of reconstruction distance and object depth position from the focal plane in experiments and theoretical calculations, (b) a focused beads' image, (*c*) hologram, and (d) the reconstructed image.

Similar experiments were performed using human lung cancer cells (NCI-H2228 ATCC® CRL-5935™), in which the nuclei were stained with propidium iodide (ThermoFisher P1304MP). The fluorescence had a peak intensity at 620 nm. We used a band-pass filter with a 650 nm $\pm$ 12.5 nm range. Fig. 6 shows that the system was capable of recording and reconstructing the nuclei of the cancer cells. The holograms of the cells were recorded by defocusing the cells by 80 μm in the axial direction.

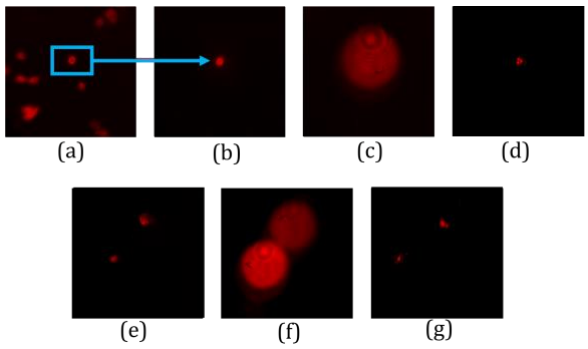

Fig. 6. Imaging and illumination of human lung cancer cells. (a, e) focused images, (b) selective illumination over a single cell, (c, f) off-axis holograms, (d, g) reconstructed images.

In this letter, we have proposed a new functional optical microscopy technique, called SIFOM, that can stimulate multiple cells located in 3D space by a phase modulation holographic method. The 3D map of cells is measured in advance by using a common-path off-axis incoherent digital holographic microscope. Simultaneous 3D observation and stimulation of biological cells will be a powerful tool in the biological field, especially in optogenetics. The performance of the proposed system was demonstrated in experiments using fluorescent beads and cancer cells. Even when the object was shifted along the axial direction, successful reconstruction was confirmed. This shows the capability of the system to perform simultaneous 3D imaging. The image degradation of the reconstructed data is due to the insufficient separation of object term from DC term in off-axis configuration. Furthermore, accurate stimulation in 3D was also possible by controlling the phase of the incoming light. This was realized by a phase-mode SLM placed before an objective lens displaying a phase pattern, which is calculated from the 3D position in the sample. This was confirmed by illuminating a single bead each time. The reconstruction results were improved compared with those of wrongly focused illumination spots.

SIFOM is expected to help in constructing artificial neural networks, especially those of mammals. In order to make a valid network, it is estimated that several hundred neurons need to be stimulated. Achieving the propagation of neural signals requires a temporal resolution of a few milliseconds. Also, artificial intelligence capable of designing a neuronal circuit in millisecond order is also required. At the current stage, SLMs have frame rates of several tens of frames per second. In order to improve the speed, binary SLMs can be employed in future studies.

Funding. Japan Society for the Promotion of Science (JSPS) KAKENHI (16J05689, 15H03580, 18H03888), and JST CREST Grant Number JPMJCR1755, Japan.

References

1. V. Gradinaru, F. Zhang, C. Ramakrishnan, J. Mattis, R. Prakash, I. Diester, and K. Deisseroth, Cell **141**, 154 (2010).
2. K. Deisseroth, Nat. Methods **8**, 26 (2011).
3. O. Yizhar, L. E. Fenno, T. J. Davidson, M. Mogri, and K. Deisseroth, Neuron **71**, 9 (2011).
4. A. M. Packer, B. Roska, and M. Häusser, Nat. Neurosci. **16**, 805 (2013).
5. C. Kim, A. Adhikari, and K. Deisseroth, Nat. Rev. Neurosci. **18**, 222 (2017).
6. www.scientificamerican.com/article/optogenetics-controlling
7. S. Bovetti, and T. Fellin, J. Neurosci. Meth. **421**, 66(2015).
8. J. Rosen, and G. Brooker, Nat. Photonics **2**, 190 (2008).
9. J. Hong, M. K. Kim, Opt. Lett. **38**, 5196 (2013).
10. T. Yanagawa, R. Abe, and Y. Hayasaki, Opt. Lett. **40**, 3312 (2015).
11. K. Watanabe, and T. Nomura, Appl. Optics **54**. A18 (2015).
12. M. Kumar, A. Vijayakumar, and J. Rosen, Scientific reports **7**, 11555 (2017).
13. J. P. Liu, T. Tahara, Y. Hayasaki, and T.C. Poon, Appl. Sci. **8**, 143 (2018).
14. X. Quan, O. Matoba, and Y. Awatsuji, Opt. Lett. **42**, 383 (2017).
15. O. Matoba, X. Quan, P. Xia, Y. Awatsuji, T. Nomura, Proc. IEEE **105**, 906 (2017).
16. E. R. Dufresne and D. G. Grier, Rev. Sci. Instrum. **69**, 1974 (1998).
17. Y. Hayasaki, M. Itoh, T. Yatagai, and N. Nishida, Opt. Rev. **6**, 24 (1999).
18. Y. Hayasaki, T. Sugimoto, A. Takita, and N. Nishida, Appl. Phys. Lett. **87**, 031101 (2005).
19. S. Hasegawa, Y. Hayasaki, and N. Nishida, Opt. Lett. **31**, 1705 (2006).

References

1. V. Gradinaru, F. Zhang, C. Ramakrishnan, J. Mattis, R. Prakash, I. Diester, and K. Deisseroth, "Molecular and cellular approaches for diversifying and extending optogenetics," Cell **141**, 154-165 (2010).
2. K. Deisseroth," Optogenetics," Nat. Methods **8**, 26 (2011).
3. O. Yizhar, L. E. Fenno, T. J. Davidson, M. Mogri, and K. Deisseroth, "Optogenetics in neural systems," Neuron **71** 9-34 (2011).
4. A. M. Packer, B. Roska, and M. Häusser, "Targeting neurons and photons for optogenetics," Nat. Neurosci. **16**, 805 (2013).
5. C. Kim, A. Adhikari, and K. Deisseroth, "Integration of optogenetics with complementary methodologies in systems neuroscience," Nat. Rev. Neurosci. **18**, 222 (2017).
6. www.scientificamerican.com/article/optogenetics-controlling
7. S. Bovetti, and T. Fellin, "Optical dissection of brain circuits with patterned illumination through the phase modulation of light," J. Neurosci. Meth. **421**, 66(2015)
8. J. Rosen, and G. Brooker, "Non-scanning motionless fluorescence three-dimensional holographic microscopy," Nat. Photonics **2**, 190 (2008).
9. J. Hong, M. K. Kim, "Single-shot self-interference incoherent digital holography using off-axis configuration," Opt. Lett. **38**, 5196-5199 (2013).
10. T. Yanagawa, R. Abe, and Y. Hayasaki, "Three-dimensional mapping of fluorescent nanoparticles using incoherent digital holography," Opt. Lett. **40**, 3312-3315 (2015).
11. K. Watanabe, and T. Nomura, "Recording spatially incoherent Fourier hologram using dual channel rotational shearing interferometer," Appl. Optics **54**. A18-A22 (2015).
12. M. Kumar, A. Vijayakumar, and J. Rosen, "Incoherent digital holograms acquired by interferenceless coded aperture correlation holography system without refractive lenses," Scientific reports **7**, 11555 (2017).
13. J. P. Liu, T. Tahara, Y. Hayasaki, and T.C. Poon, "Incoherent Digital Holography: A Review," Appl. Sci. **8**, 143 (2018).
14. X. Quan, O. Matoba, and Y. Awatsuji, "Single-shot incoherent digital holography using a dual-focusing lens with diffraction gratings," Opt. Lett. **42**, 383-386 (2017).
15. O. Matoba, X. Quan, P. Xia, Y. Awatsuji, T. Nomura, "Multimodal imaging based on digital holography," Proc. IEEE **105**, 906-923 (2017).
16. E. R. Dufresne and D. G. Grier, "Optical tweezers arrays and optical substrates created with diffractive optics," Rev. Sci. Instrum. **69**, 1974-1977 (1998).
17. Y. Hayasaki, M. Itoh, T. Yatagai, and N. Nishida, "Nonmechanical optical manipulation of microparticle using spatial light modulator," Opt. Rev. **6**, 24-27 (1999).
18. Y. Hayasaki, T. Sugimoto, A. Takita, and N. Nishida, "Variable holographic femtosecond laser processing by use of a spatial light modulator," Appl. Phys. Lett. **87**, 031101 (2005).
19. S. Hasegawa, Y. Hayasaki, and N. Nishida, "Holographic femtosecond laser processing with multiplexed phase Fresnel lenses," Opt. Lett. **31**, 1705-1707 (2006).